2024 European Control Conference (ECC)
June 25-28, 2024. Stockholm, Sweden

Learning Compensation of the State-Dependent Transmission Errors in Rack-and-Pinion Drives

Lukas Steinle[1], Valentin Leipe[1], Armin Lechler[1], and Alexander Verl[1], *Member, IEEE*

***Abstract*— Rack-and-pinion drives are commonly used in large machine tools to provide linear motion of heavy loads over long travel distances. A key concern in this context is the achievable path accuracy, which is limited by assembly and manufacturing tolerances of the gearing components in conjunction with load-dependent deformation and the inherent backlash of the system. To address this issue, this paper presents a method for robust modeling of the individual and state-dependent transmission errors of a drive utilizing a two-stage machine learning approach. Based on this, the position control is extended to include an error compensation, which suppresses the modeled deviations in the mechanical system including the position-dependent backlash. The achievable increase in path accuracy as well as the robustness of the approach are evaluated and quantified by an experimental validation on a system with industry standard components.**

I. Introduction

The demands on modern production equipment are steadily increasing, with machine tools being particularly impacted by this. The minimization of cycle times necessitates high dynamics with simultaneously increasing requirements on manufacturing quality and accuracy. The installed drive systems are of decisive importance in this context [1]. To provide linear motion of high loads over long travel distances, rack-and-pinion drives (RPDs) are commonly utilized. These have the distinct advantage over ball screw drives that stiffness and moving inertia are independent of the travel length [2]. This aspect, combined with high cost efficiency and scalability, renders RPDs the preferred choice for large and heavy machinery [3].

A major disadvantage, however, is the inferior positioning and path accuracy compared to other drive systems. Inaccuracies in the mechanical drive train and the backlash immanent in the system lead to deviations of the table position even when a linear measuring system is utilized to close the position control loop for improved accuracy [4]. To increase the versatility of machines with RPDs and reduce rework of parts, efforts are being made to reduce the influence of these errors between the input and output of the drive train, commonly referred to as transmission errors (TEs) [5].

Existing works on this subject mostly investigate gear pairs and approach the problem primarily from a gear design perspective [6]–[8]. In the context of RPDs, redundant electrically preloaded drives with an adapted control structure are often used to suppress backlash [9]. However, this is associated with considerable additional costs and enlarged installation space. Regarding the control-based compensation of backlash in position-controlled drives, several approaches exist that do not explicitly address RPDs and instead use simplified test setups. However, these are often acknowledged by the authors to lack robustness to parameter uncertainties concerning the magnitude of backlash [10]–[12] which hinders the industrial use on RPDs.

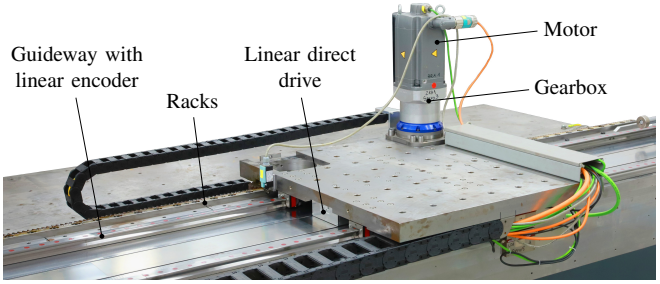

Fig. 1: RPD test bench used for the measurements.

This paper aims to increase the accuracy of single drive RPDs with linear measuring systems by comprehensive compensation of the state-dependent TEs including backlash for all operating conditions. In prior work, the composition of TEs in RPDs and their impact on path accuracy have been investigated through measurements [4] and a basic methodology for adaptive error compensation at constant travel velocities has been presented [13]. Leveraging the knowledge gained, this paper proposes a novel approach to a learning model of the TEs of RPDs in order to achieve satisfactory robustness and reliability. Furthermore, a compensation of the modeled errors in the position control of the drive for all operating conditions is presented. All measurement data in this publication, including variables that are not displayed and supplementary data, can be accessed in [14].

II. Characteristics of Transmission Errors in Rack-and-Pinion Drives

In the following, the transmission characteristics of RPDs are explained based on measurements using a test bench that is shown in Fig. 1 and the authors described in detail in a previous publication [4]. The installed RPD has a module m of $4\,\mathrm{mm}$ with a number of teeth n_t of 20 and a pinion pitch diameter d_p of $84.882\,\mathrm{mm}$. It is driven by a servo motor via a high-precision two-stage planetary gearbox with a transmission factor i_PG of 16 and it moves a table mass m_T of $400\,\mathrm{kg}$. For position measurement, the motor

This work was funded by the Deutsche Forschungsgemeinschaft (DFG, German Research Foundation), Project No. 447112572 and 521502188. The authors gratefully acknowledge the support by DFG.

[1] The authors are with the Institute for Control Engineering of Machine Tools and Manufacturing Units, University of Stuttgart, Stuttgart 70174, Germany, lukas.steinle@isw.uni-stuttgart.de

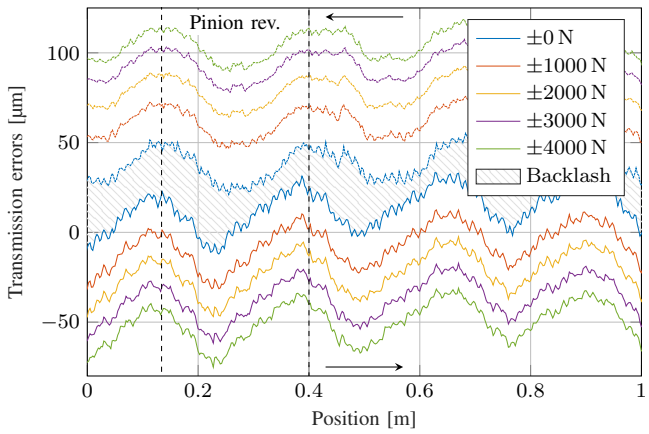

Fig. 2: TEs of the examined RPD in both directions under varying load.

encoder and a linear measuring system integrated in the guideways are utilized. The mechanical components as well as the drive components including the inverter are industry standard components. A notable feature of the test bench is a redundant linear direct drive (LDD), which is force-controlled and allows the application of external disturbance forces to the RPD. The test bench is operated through a dedicated control computer, which is connected to the drives via field bus and handles the position control and acquisition of measurement data.

As previously mentioned, TEs in the context of RPDs denote the difference

$$TE = x_\mathrm{T} - x_\mathrm{M} = x_\mathrm{T} - \frac{\theta_\mathrm{M}\, d_\mathrm{P}}{2 i_\mathrm{PG}} \tag{1}$$

between the table position x_T and the linear motor position x_M derived from the motor angle θ_M. To analyze them, the drive is moved at a low velocity of $10\,\mathrm{mm/s}$ to exclude dynamic effects, while varying external forces against the direction of motion are applied by the LDD. Fig. 2 shows the acquired error curves with the positive direction of motion in the lower part and the negative in the upper part. A load dependency of the TEs is evident. The error curves observed without external load neglecting friction are commonly referred to as geometric errors TE_geo [15]. In the case of RPDs they are mainly composed of three components. First, a superimposed drift is apparent, which is primarily a result of manufacturing and assembly tolerances of the rack elements. A low-frequency oscillation with a period corresponding to the pinion circumference and an amplitude of circa $25\,\mu\mathrm{m}$ is superimposed to this, mainly caused by runout errors of the pinion and in the gearbox [4]. The third component is a higher-frequency oscillation with a lower amplitude between $4\,\mu\mathrm{m}$ and $8\,\mu\mathrm{m}$ whose period corresponds to the tooth meshing. These errors result from deviations of the tooth flank geometry from an ideal involute due to manufacturing tolerances as well as intentionally applied profile modifications, for example to increase the load capacity [16]. Predominantly this last error component exhibits a pronounced load-dependent alteration, with the amplitude decreasing with increasing load. The reason for this is the deformation of the tooth flanks and the resulting change in the contact conditions in conjunction with the profile modifications just mentioned. These deformations TE_def that are added on the geometric errors are typically referred to as static load-induced elastic errors [15]. It should be noted that these errors can only be systematically examined on the test setup using the LDD as a load. When commissioning an actual machine, only the geometric errors can be measured directly.

Considering the direction of travel, it is evident that while the general pattern of the TEs is similar for both directions, there are nevertheless significant discrepancies. This can be explained by the individual manufacturing errors of the tooth flanks for the respective direction of travel as well as changed contact conditions in the pinion shaft bearings [8]. This is also evident when examining the geometric backlash, which is characteristic for RPDs and cannot be completely eliminated by design [5]. It is visualized in Fig. 2 through the highlighted area between the two no-load error curves. It is evident that the magnitude of the backlash is not constant along the travel path, but varies in analogy to the previous explanations due to manufacturing and assembly tolerances. As mentioned in Sec. I, this variation poses a challenge for the compensation of the backlash.

To summarize, the state-dependent TEs including the backlash of RPDs are heavily influenced by manufacturing and assembly tolerances and are thus highly individual to each drive as well as to direction of travel.

III. Negative Effects of Transmission Errors on the Path Accuracy

In the following, building on the findings presented in the previous section, the influence of the TEs on the path accuracy of position-controlled RPDs with linear measuring systems is derived theoretically and validated by measurement. The theoretical background does not aim at a comprehensive modeling, but at a practical approach to estimate the expected path errors utilizing typically known parameters. Since the explanations refer to a single axis, the position control error and path error or path tracking error are equivalent.

The position control of feed axes is generally implemented by means of a cascade control [1]. A common simplification is the modeling of the mechanical subsystem as a two-mass oscillator [17]. Since it is primarily the position control loop that is of interest when examining the impact of the TEs, further simplifications can be made. As the bandwidth of the current control loop is assumed to be substantially higher than that of the superimposed control loops, the motor torque T_M is considered to equal the desired torque T_d. Adding to this, given a well-damped tuning of the velocity controller and smooth trajectories, it can be assumed that the elasticity of the system is not excited. Thus, the two inertias of the two-mass oscillator can be aggregated to a combined inertia J_s as to their effect on the position control loop [2], [18]. As a result, the equivalent schematic of the position-controlled system shown in Fig. 3 is obtained.

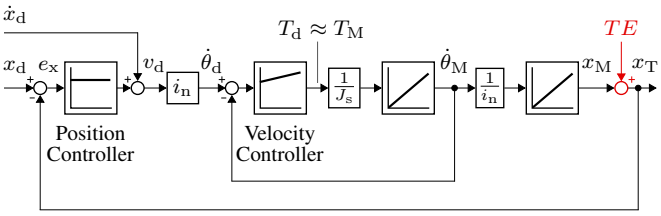

Fig. 3: Schematic of the position controlled RPD with TEs as output disturbance.

The setpoint of the PI velocity controller v_d is computed by the P position controller combined with a commonly added velocity feedforward. Due to the use of a linear measuring system, the position controller and its output refer to the linear axis position. Therefore, the linear set velocity must be converted into the rotational desired motor velocity $\dot{\theta}_\mathrm{d}$ prior to the velocity controller. In the state of the art, this is done using the nominal transmission ratio i_n. The set torque computed by the velocity controller accelerates the inertia of the system. When the rotational motor velocity $\dot{\theta}_\mathrm{M}$ is then reconverted into the linear table velocity, again using i_n, the real system now deviates from the idealized model shown. The mechanical inaccuracies discussed in the previous section result in deviations from the nominal transmission ratio and consequently in the measured TEs. To account for this in the model, in accordance with their definition (1), the TEs are incorporated as an output disturbance, representing the difference between linear motor position and the table position.

For the test bench, the velocity controller was set to a gain K_p of $12.4\,\mathrm{Nm\,s/rad}$ and an integrator time constant T_n of $3.05\,\mathrm{ms}$ for maximum dynamics following the standard procedure for Siemens drive controllers [19]. The position controller was then set to be overshoot-free (aperiodic-loop), resulting in a gain of K_v of $23\,1/\mathrm{s}$ [18]. Based on the outlined control scheme, the open-loop position control transfer function

$$G_\mathrm{pc,OL} = \left.\frac{x_\mathrm{T}}{x_\mathrm{d}}\right|_{TE=0} = \frac{K_\mathrm{v}K_\mathrm{p}(T_\mathrm{n}s+1)}{s(J_\mathrm{s}T_\mathrm{n}s^2+K_\mathrm{p}T_\mathrm{n}s+K_\mathrm{p})} \tag{2}$$

from the desired position x_d to the table position can be derived. Subsequently, the disturbance transfer function

$$G_\mathrm{d,CL}=\frac{e_\mathrm{x}}{TE}=-\frac{\frac{J_\mathrm{s}T_\mathrm{n}}{K_\mathrm{p}}s^3+T_\mathrm{n}s^2+s}{\frac{J_\mathrm{s}T_\mathrm{n}}{K_\mathrm{p}}s^3+T_\mathrm{n}s^2+(1+K_\mathrm{v}T_\mathrm{n})s+K_\mathrm{v}} \tag{3}$$

from the TEs to the closed-loop position control error e_x is obtained. It is a third-order transfer function with high-pass characteristics, which means high-frequency error components are represented in the path error nearly unaltered. For lower frequency components, the gain of the position control loop K_v is decisive for the suppression of the errors. The dynamics of the velocity control loop are of minor significance under the assumptions made.

Using (3) and the measured TEs shown in Fig. 2, the expected path errors are calculated for different velocities with no external load and compared in Fig. 4 with respective

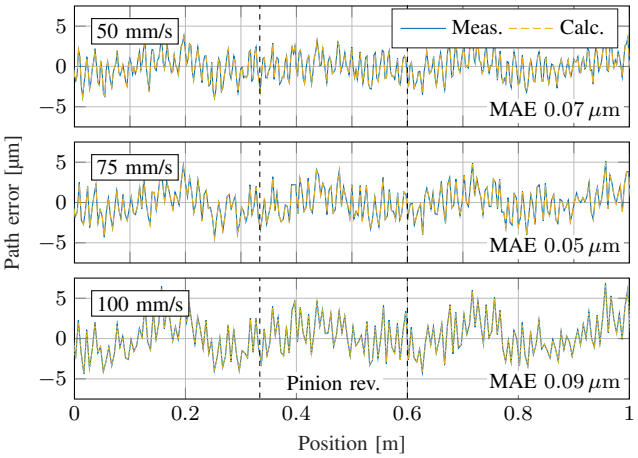

Fig. 4: Comparison of calculated and measured path errors.

measurement data. This shows a high concordance between the calculated and the measured path errors with a mean absolute error (MAE) below $0.1\,\mu\mathrm{m}$ for all cases. As was derived from the transfer function, primarily the high-frequency TEs with tooth meshing frequency appear in the path error. The lower frequency oscillations are substantially reduced and the position drift completely suppressed by the position controller. Since the TEs depend on the position of the drive, their temporal frequency is variable and depends on the velocity. Higher velocities yield higher frequencies and thus poorer suppression.

It can be stated, that while the negative influence of the TEs of RPDs on the path accuracy can be significantly reduced by feeding back the measured table position, it cannot be completely negated. In particular, high-frequency errors with tooth meshing frequency are present in the path error, leading to unsatisfactory surface quality of workpieces and, due to their periodicity, to vibration excitation of the machine structure.

IV. Modeling the Transmission Errors

To address this issue and develop an error compensation for the position control, it is first necessary to represent the state-dependent TEs in models. The geometric TEs can be stored in lookup tables during commissioning of the drive using the available measuring systems. However, compensation based only on this data is not sufficient and can even worsen the path accuracy over a large part of the operating range, as shown in previous works [13]. To prevent this, the load-dependent deformation must also be taken into account. But as mentioned in the previous sections, this poses a considerable challenge. Lacking the ability to selectively apply loads, the deformations cannot be systematically obtained on a real machine. Analytical or numerical methods that are commonly used to predict elastic deformations cannot provide sufficient accuracy for this application due to the high degree of individuality. Instead, the deviations that actually occur can only be acquired during operation, for example during commissioning and testing of the machine.

However, the unstructured and incomplete composition of the data is challenging due to the dependency on motion profiles and process forces. Regression methods from the field of machine learning (ML) can be applied to process this data and generate models that can be used for compensation.

For this purpose, the required data processing is elaborated to begin with. To eliminate the velocity dependent scaling of the position-fixed TEs in the time domain and moreover to reduce the amount of data, all measurements are interpolated over the drive position with a fixed step size of $50\,\mu\mathrm{m}$. The TEs are then calculated and, by comparison with the previously measured geometric errors, the deformations TE_{def} under the momentary load in the form of the motor torque are determined. After removing constant offsets, the curves are then smoothed by low-pass filters with a cut-off frequency three times higher than the tooth meshing frequency. An efficient method to minimize the complexity of regression models is the addition of indirect training data [20]. In the case at hand, the gear meshing state between rack and pinion, that indicates the expected periodicity of the deformations, is a useful supplement. Therefore, for each tooth of the pinion j a variable M_j is added, which reflects its meshing through a bump function

$$M_j = \begin{cases} \exp\left(\frac{\eta_j^2}{\eta_j^2-1}\right) & \eta_j \in (-1,1) \\ 0 & \text{otherwise} \end{cases} \tag{4}$$

with

$$\eta_j = \frac{2}{\varepsilon}\ \mathrm{mod}\left(\frac{x_{\mathrm{T}}\, n_{\mathrm{t}}}{\pi d_{\mathrm{p}}} - j,\ n_{\mathrm{t}}\right) - 1 \tag{5}$$

based on the contact ratio of the gearing ε, with $\mathrm{mod}()$ representing a modulo operation [13].

Regression models are then trained on the basis of the processed input variables (x_{T}, T_{M}, M_j), with both directions of travel being handled separately. A common difficulty with ML-based approaches in the context of manufacturing is the lack of comprehensive data [21]. To nonetheless ensure robust performance, sufficient generalization of the relations derived from the limited data to the state space is required. At the same time, effective error compensation requires high accuracy of the models. However, there is a conflict between these two requirements in the optimization of regression models, known as bias-variance tradeoff [22].

To overcome this problem, a modeling approach optimized for the specific characteristics of TEs is introduced. As stated before, the TEs and the load-dependent deformations are inherently periodic, but in the presence of local variations due to uncertainties. To effectively model these different aspects, two stacked models are used, as shown in Fig. 5. In a first modeling step, a neural network (NN) is trained only relying on the load and the tooth meshing, but not the drive position. This forces the regression to generalize over the travel range and results in only periodic and recurring effects being represented. Thus, only the general elasticities of components and the tooth flanks are modeled, while localized effects are neglected. In this case, back-propagation networks with two layers and rectified linear activation functions (ReLU) trained by the Adam algorithm are used [23], [24]. The performance in form of the mean absolute error during training is continuously monitored against a validation set previously randomly extracted from the training data to ensure generalization capabilities and to avoid overfitting. This is aided by the implementation of dropout layers that randomly disable a portion of each fully connected layer during each training step and have a strong regularizing effect [23]. To minimize the configuration effort, the dropout rate, the number of nodes and the learning rate are determined using a hyperband optimization [25].

After training the NN, its predictions are calculated for the entire data set and the residual error to the measured deformations is obtained. These residual errors, which correspond to the localized non-periodic deviations, are then processed by the second model, that receives the drive position instead of the meshing information as an input. The basic principle of this approach resembles that of gradient boosting, albeit only involving two models [22]. Since the priority in this second step is to represent errors that have already appeared with a high degree of accuracy, while disregarding generalization, bagged regression trees (BRT) based on the CART algorithm are applied [26], [27]. They feature high accuracy with fast training and reliable convergence, while coping well with fragmented data. To minimize the configuration effort, the relevant parameters in form of the number of trees, their maximum depth and the minimum leaf size are determined by a grid search using cross validation in this case [28].

Subsequently, the two models are combined as shown in Fig. 5 and their predictions are summarized. The developed approach has several advantages. First, the trade-off between high accuracy and generalization can be largely resolved, as will be validated in Sec. VI. The dedicated use of NNs to represent the general compliance offers further benefits. Trained NNs can be updated with new data without needing to repeat the entire training [23]. This way, models pre-trained on data of other drives or simulation data, e.g. FEM, can be used as the basis for new drives, thus potentially reducing the amount of data and training time required. The approach is also beneficial in terms of possible model degradation due to alterations of the system, e.g. wear, which in practice is one of the main reasons for insufficient performance of ML-based solutions [29]. Since this primarily affects the local deviations, while the general elasticity remains unchanged, only the fast-trainable regression trees have to be updated.

To validate the capability of the developed approach, a

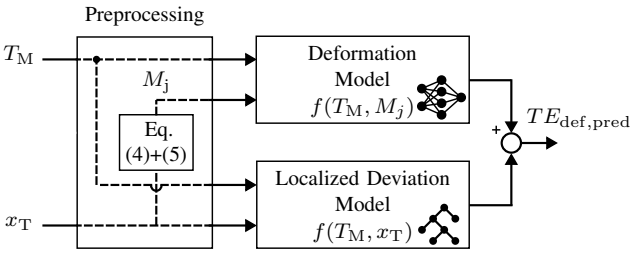

Fig. 5: Stacked architecture to model the state-dependent deformations.

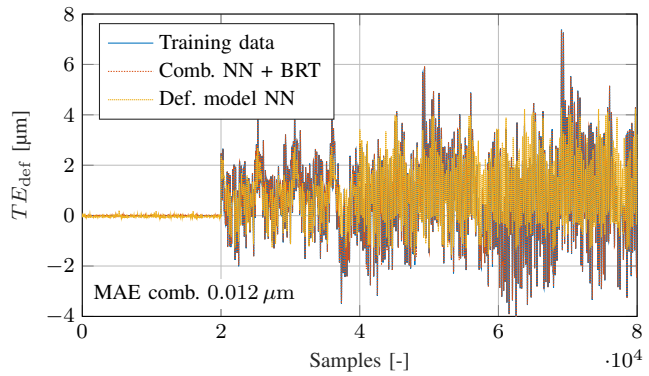

Fig. 6: Combined model prediction and contribution of the NN over the training data.

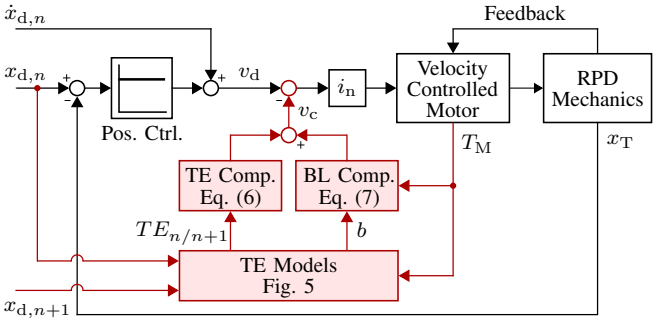

Fig. 7: Control scheme with TE and backlash (BL) compensation.

greatly reduced training data set, analogous to Fig. 2, but including only loads up to 3000 N is used in this paper. The following results refer to the positive direction of travel, those of the negative are comparable. Fig. 6 shows the predictions over the training data set, illustrating the prediction accuracy of the combination of both models with a MAE of $0.012\,\mu\mathrm{m}$ as well as the contribution of the NN deformation model, which accounts for $42\,\%$ of the total output in this case. It should be noted that this ratio highly depends on the properties of the examined system and the magnitude of local deviations, that are represented by the BRT.

V. Error Compensation

The approach developed in the previous section enables the prediction of the state-dependent TEs. On this basis, an error compensation is integrated into the existing cascade control, as shown in Fig. 7, where the velocity controlled motor is a simplified representation of the motor controlled by a cascaded current and velocity control, as described in Sec. III. The basic idea is to introduce a correction velocity v_{c} which offsets the deviations of the system from the nominal transmission ratio caused by the TEs. For this purpose, the error TE_n given by the models for the current position $x_{\mathrm{d},n}$ and motor torque is first obtained. Then, assuming the load remains unchanged until the next time step, the error TE_{n+1} at the future position $x_{\mathrm{d},n+1}$, which is obtained from the trajectory planning look-ahead, is determined. The assumption of a piece-wise constant load over the comparatively high sampling rate is reasonable here since the low mechanical eigenfrequencies of large machines and the resulting low-pass characteristic strongly smooth the impact of process-related load changes on the drives anyway [3]. By comparing the momentary and future error and taking into account the sample time of the compensation $t_{\mathrm{s,c}} = 5\,\mathrm{ms}$ the TE correction velocity

$$v_{\mathrm{c,TE}} = \frac{TE_{n+1} - TE_n}{t_{\mathrm{s,c}}} \tag{6}$$

can be calculated.

The direction of travel respectively the tooth flank contact is determined based on the motor torque and the associated geometric error curve and deformation model are applied. A change of tooth flanks and the resulting occurrence of backlash is detected by a sign change of the motor torque after deducting the friction and acceleration torque of the drive train. The magnitude of the backlash b at the current position can then be determined using the TE models. This way, however, the backlash is represented as a discontinuous step. A compensation cannot completely offset this, as saturation limitations must be taken into account and an excitation of the system must be avoided [12]. For this reason, the backlash is smoothed by a sigmoid like smooth step function [30] and is then derived to obtain the correction velocity

$$v_{\mathrm{c,BL}} = \frac{\partial}{\partial t}\, b \cdot \begin{cases} 0 & t \le 0 \\ 3(t/t_{\mathrm{ss}})^2 - 2(t/t_{\mathrm{ss}})^3 & 0 \le t \le t_{\mathrm{ss}} \\ 1 & t_{\mathrm{ss}} \le t \end{cases}. \tag{7}$$

This way, the compensation is spread over the time interval t_{ss}, that was experimentally determined to $35\,\mathrm{ms}$. The total correction velocity v_{c} subsequently is the sum of the two components for compensation of the TEs and the backlash.

The underlying principle of the compensation is implemented as a feedforward path, which continuously computes the correction velocity based on the planned trajectory. As illustrated in Fig. 7, a feedback of the motor torque exists, however, there is no direct feed-through to the output of the compensation. Instead, the motor torque is used only indirectly as a state variable for the error models and backlash detection, with its range of effect on the correction velocity strictly limited by the models. This ensures that the parameters and stability characteristics of the position control loop remain unchanged.

VI. Experimental Validation

After the modeling of the TEs and the compensation have been presented, their functionality is validated in the following on the test bench introduced in Sec. II. For this purpose, an exemplary trajectory in the form of a sinusoidal profile including a change of direction is examined. Fig. 8 shows the TEs, a comparison of the path errors and the correction velocity v_{c} calculated by the compensation. It is evident that the path errors caused by the TEs are substantially reduced over the entire velocity range for both directions. Moreover, the path error during the change of direction due to the backlash can be largely eliminated. The remaining sinusoidal

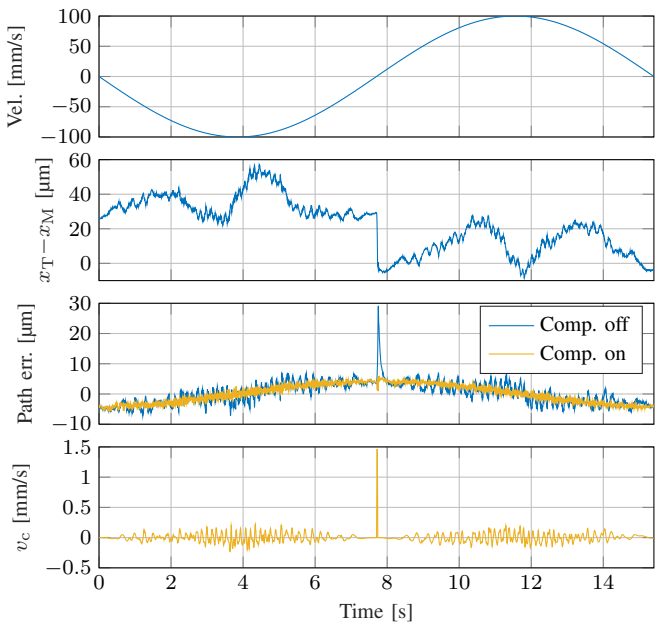

Fig. 8: Compensation of the TEs and backlash for a sinusoidal trajectory.

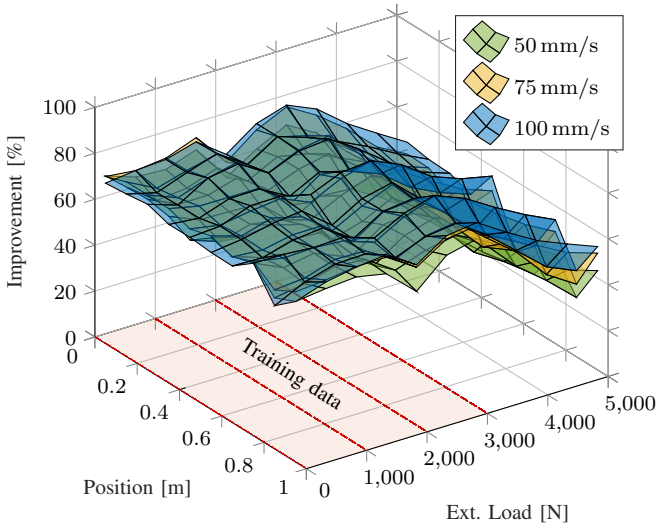

Fig. 9: Improvement of path accuracy by the compensation for varying loads and velocities.

error can mainly be attributed to the lack of an acceleration feedforward, whose implementation is not trivial for RPDs and is subject of other research.

In addition to the overall functionality, the robustness of the approach is evaluated by validating the generalization capabilities of the models trained with a very limited data set in Sec. IV. This was done by repeatedly cycling the travel range at constant velocity, increasing the load by 500 N in each pass up to a maximum of 5000 N. Each pass was performed once without and once with the compensation, quantifying its performance by the percentage improvement of the MAE of the path error in sections of 100 mm. The entire series of measurements was repeated for three different velocities. Fig. 9 shows the results obtained for the positive direction of travel, the negative is similar. Within the known load range from the training data, the performance of the compensation is reasonably consistent, even for loads not included in the training data set, which validates the generalization capabilities of the modeling approach. In this area the compensation can achieve a satisfactory improvement of the path accuracy between 50 % and 75 % for all loads and velocities. For the loads above 3000 N, which is outside the training data, the performance deteriorates as expected. However, due to the efforts to ensure sufficient model generalization, an improvement of at least 25 % can still be achieved. The average of all measurement points yields an improvement of 66 %.

For the validation, reference measurements were performed without compensation. However, it is also possible to estimate the path errors that would occur without compensation while it is active by applying the transfer function (3) on the measured TEs, as explained in Sec. III. This allows a continuous monitoring of the performance of the compensation during operation and the detection of states where the model quality is insufficient. This information can then be used to trigger automated retraining of the models with updated data sets or to diagnose changes in the system behaviour as part of a condition monitoring.

VII. Conclusion

In this paper, a novel approach for a learning compensation of transmission errors including backlash in rack-and-pinion-drives using stacked machine learning models is presented. Inaccuracies due to assembly and manufacturing tolerances, elastic deformation of the tooth flanks and the inherent backlash in the drive train limit the achievable path accuracy of rack-and-pinion-drives. Despite the use of linear measuring systems, path errors remain due to the limited bandwidth of the position control.

Modeling the transmission errors as an output disturbance, a simple theoretic relationship is derived, that gives an estimation of the path errors to be expected. The transmission errors and backlash are highly individual as well as position- and load-dependent, rendering identification and modeling difficult. In the proposed approach, the transmission errors are divided into geometric errors that are acquired during commissioning and deformation errors, that can only be observed during operation and are modeled by real-time capable regression models. To be suitable for use in practice, the models must provide reliable results given a limited amount of training data. To ensure this, a two-stage training process is developed utilizing a neural network to model the general elasticity of the gearing and a regression tree ensemble to account for localized deviations. Based on the error models, a compensation is integrated into the established cascade control, that compensates for the state-dependent transmission errors by applying a correction velocity. The occurrence of backlash is detected and also compensated for, taking into account the limited system dynamics. A concept for automated monitoring of the compensation performance

and consequent updating of the regression models is presented.

The developed approach is experimentally validated on a test bench. The performance of the compensation for accelerated motion including backlash is investigated as well as the robustness and generalization capabilities of the error models. It is demonstrated that the specialized modeling approach can achieve robust performance even for unknown system states and the compensation reduces the path errors by an average of $66\,\%$ in the investigated scenarios.

Future work includes transferring the approach to commonly used electrically preloaded dual drive systems and validating the compensation in actual manufacturing processes and other motion profiles.

REFERENCES

[1] Y. Altintas, A. Verl, C. Brecher, L. Uriarte, and G. Pritschow, "Machine tool feed drives," *CIRP Annals*, vol. 60, no. 2, pp. 779–796, 2011.

[2] C. Brecher and M. Weck, *Machine Tools Production Systems 3*. Wiesbaden: Springer Fachmedien Wiesbaden, 2022.

[3] L. Uriarte *et al.*, "Machine tools for large parts," *CIRP Annals*, vol. 62, no. 2, pp. 731–750, 2013.

[4] L. Steinle, A. Lechler, M. Neubauer, and A. Verl, "Experimental investigation into the implications of transmission errors for rack-and-pinion drives," *Production Engineering*, vol. 16, no. 4, pp. 453–463, 2022.

[5] V. Vullo, *Gears: Volume 1: Geometric and Kinematic Design*, 1st ed. Cham: Springer International Publishing and Imprint Springer, 2020, vol. 10.

[6] E. Rocca and R. Russo, "Theoretical and experimental investigation into the influence of the periodic backlash fluctuations on the gear rattle," *Journal of Sound and Vibration*, vol. 330, no. 20, pp. 4738–4752, 2011.

[7] Z. Chen, M. Zeng, and A. Fuentes-Aznar, "Geometric design, meshing simulation, and stress analysis of pure rolling rack and pinion mechanisms," *Journal of Mechanical Design*, vol. 142, no. 3, 2020.

[8] V. Roda-Casanova and F. Sanchez-Marin, "Contribution of the deflection of tapered roller bearings to the misalignment of the pinion in a pinion-rack transmission," *Mechanism and Machine Theory*, vol. 109, pp. 78–94, 2017.

[9] T. Engelberth, S. Apprich, J. Friedrich, D. Coupek, and A. Lechler, "Properties of electrically preloaded rack-and-pinion drives," *Production Engineering*, vol. 9, no. 2, pp. 269–276, 2015.

[10] A. Lagerberg and B. Egardt, "Backlash estimation with application to automotive powertrains," *IEEE Transactions on Control Systems Technology*, vol. 15, no. 3, pp. 483–493, 2007.

[11] P. Rostalski, T. Besselmann, M. Barić, F. van Belzen, and M. Morari, "A hybrid approach to modelling, control and state estimation of mechanical systems with backlash," *International Journal of Control*, vol. 80, no. 11, pp. 1729–1740, 2007.

[12] S. Yamada and H. Fujimoto, "Precise joint torque control method for two-inertia system with backlash using load-side encoder," *IEEJ Journal of Industry Applications*, vol. 8, no. 1, pp. 75–83, 2019.

[13] A. Verl and L. Steinle, "Adaptive compensation of the transmission errors in rack-and-pinion drives," *CIRP Annals*, vol. 71, no. 1, pp. 345–348, 2022.

[14] L. Steinle, "Replication Data for: Learning Compensation of the State-Dependent Transmission Errors in Rack-and-Pinion Drives," https://doi.org/10.18419/darus-3759, DaRUS, 2024.

[15] W. Gao *et al.*, "Machine tool calibration: Measurement, modeling, and compensation of machine tool errors," *International Journal of Machine Tools and Manufacture*, vol. 187, 2023.

[16] U. Kissling, "Effects of profile corrections on peak-to-peak transmission error," *Gear technology*, vol. 27, no. 5, pp. 52–61, 2010.

[17] W. Leonhard, *Control of electrical drives*, 3rd ed., ser. Power systems. Berlin and Heidelberg: Springer, 2001.

[18] O. Zirn, "Machine tool analysis: modelling, simulation and control of machine tool manipulators," Habilitation Thesis, ETH Zurich, 2008.

[19] Siemens AG, "Drive optimization guide: V2.1," 2019, Accessed: Sep. 6, 2023. [Online]. Available: https://publikacje.siemens-info.com/pdf/677/

[20] A. Burkov, *Machine learning engineering*. Quebec City, Canada: True Positive Inc, 2020.

[21] T. Chen *et al.*, "Machine learning in manufacturing towards industry 4.0: From 'for now' to 'four-know'," *Applied Sciences*, vol. 13, no. 3, p. 1903, 2023.

[22] T. Hastie, R. Tibshirani, and J. Friedman, *The Elements of Statistical Learning*. New York, NY: Springer New York, 2009.

[23] C. C. Aggarwal, *Neural Networks and Deep Learning*. Cham: Springer International Publishing, 2018.

[24] D. P. Kingma and J. Ba, "Adam: A method for stochastic optimization," *arXiv preprint arXiv:1412.6980*, 2014.

[25] L. Li, K. Jamieson, G. DeSalvo, A. Rostamizadeh, and A. Talwalkar, "Hyperband: A novel bandit-based approach to hyperparameter optimization," *J. Mach. Learn. Res.*, vol. 18, no. 1, pp. 6765–6816, 2017.

[26] L. Breiman, "Bagging predictors," *Machine Learning*, vol. 24, no. 2, pp. 123–140, 1996.

[27] W.-Y. Loh, "Classification and regression trees," *WIREs Data Mining and Knowledge Discovery*, vol. 1, no. 1, pp. 14–23, 2011.

[28] C. M. Bishop, *Pattern recognition and machine learning*, ser. Computer science. New York, NY: Springer, 2006.

[29] D. Vela, A. Sharp, R. Zhang, T. Nguyen, A. Hoang, and O. S. Pianykh, "Temporal quality degradation in ai models," *Scientific reports*, vol. 12, no. 1, p. 11654, 2022.

[30] B. Mark and J. Hart, *Texturing & modeling: A procedural approach*, 3rd ed., ser. The Morgan Kaufmann series in computer graphics and geometric modeling. Amsterdam: Morgan Kaufmann, 2003.